Composite Pd membranes for hydrogen separation

by

Lester Li
Amanda E. Young

A Major Qualifying Project
Submitted to the Faculty of the
WORCESTER POLYTECHNIC INSTITUTE
in partial fulfillment of the requirements for the
Degree of Bachelor of Science
in
Chemical Engineering

April 30, 2009

Lester Li

Amanda E. Young

APPROVED:

Dr. Yi Hua Ma, Advisor

ABSTRACT

The effects of support material on the permeation characteristics of composite Pd membranes were examined. Membranes supported on uncoated porous stainless steel (USS) and zirconia (ZrO_2) coated porous stainless steel were prepared by electroless plating. The reduced and uniform pore size of the ZrO_2 made it possible to obtain a 6.9 μm thick Pd layer, while that of the USS was 54.1 μm. H_2 flux testing conducted between 300-400^oC found that the membranes followed Sieverts Law. The thin Pd layer allowed for a higher flux, while the greater thickness of the USS membrane allowed for a higher selectivity. The reduced pore size of the ZrO_2 increased the mass transfer resistance, resulting in a lower percentage of the maximum achievable permeability.

ACKNOWLEDGEMENTS

谢谢你, Professor Yi Hua Ma, for your guidance and patience with us. You not only motivated us to do better, but took the time to teach and explain to ensure we thoroughly understood the concepts.

We would also like to especially thank Professor M. Engin Ayturk. We would have been unable to complete this project without your help and knowledge. Thank you to the CIMS group for their continued support of our project.

TABLE OF CONTENTS

TABLE OF FIGURES

TABLE OF TABLES

CHAPTER 1 INTRODUCTION

In 1866, Sir Thomas Graham discovered palladium's (Pd) selectivity towards hydrogen. However, it was not until the recent push towards alternative fuels that the use of Pd membrane to purify hydrogen was studied extensively.

Pd's high selectivity towards hydrogen has gained its favor as the element of choice in the purification of hydrogen. Currently, hydrogen gas is most commonly produced through methane steam reforming. For this method of production, methane is mixed with steam, and reacted to form hydrogen gas. While using this method to produce hydrogen gas in large quantities is feasible, the product contains impurities. The use of a membrane that is selectively permeable to hydrogen would not only yield a highly pure gas, but if used in conjunction with the steam reforming reaction, could also drive the reaction forward with higher efficiency as product is removed. While the physical properties of Pd are promising for its use in hydrogen production, several hurdles still need to be overcome. In general, the production of dense Pd membranes is focused on improving two areas: (a) increasing and verifying the lifespan of the membrane and (b) increasing the flux of hydrogen through the membrane.

There are several methods that are being used in the production of Pd membranes, including, but not limited to, plasma sputtering, magnetron sputtering, flame spraying, and electroless plating. All the processes have the same end goal of producing a layer of Pd that is not only defect-free and uniform, but also extremely thin in order to promote a higher flux, while remaining stable enough to have a long lifespan. The flux of hydrogen through palladium is inversely proportional to the thickness, leading to an interest in thinner membranes (Wang, et al., 2004). However, the wide use of membranes is still held back by the high cost of Pd coupled with remaining concerns about the lifespan of the membranes. Thinner membranes will have reduced mechanical strength and any defects will be exploited at elevated temperatures and pressures. This research will utilized the electroless plating process to produce dense membranes. This process has been shown to produce thin membranes that are not only dense and uniform, but also defect-free (Mardilovich, et al., 1998).

In order to combat the price and ensure adequate mechanical strength, and therefore durability, of the membrane, Pd is often supported on a porous substrate and/or alloyed with silver (Ag). The study of the long-term diffusion characteristics of porous stainless steel (PSS)-supported Pd and Pd/Alloy membranes has shown that the stability of the membranes can be limited by the occurrence of intermetallic diffusion from the porous metal support into the Pd layer. At the high operating temperature of the methane

reforming reaction, intermetallic diffusion is significant. The action of diffusion causes the non-selective stainless steel to diffuse into the hydrogen-selective Pd, leading to the reduction of hydrogen flux through Pd and eventually to the failure of the membrane. Research into the prevention of intermetallic diffusion has been conducted by implementing an oxide layer between the support and the plated material (Ayturk, et al., 2006).

A way to further avoid the diffusion completely is to plate the membrane on a porous ceramic support. Ceramics do not react with metals and have proven to be a suitable substitute to stainless steel in some cases (Richerson, 2006). However, while the chemical properties of a ceramic support and the Pd membrane do not interact, the mechanical properties present another issue. At the operating temperature of the methane reforming process, the coefficients of thermal expansion for the ceramic support and the Pd membrane are considerably different. The thermal expansion coefficient of Pd is roughly $1.2 \times 10^{-5}/^{o}C$ and that of cast stainless steel is $1.9 \times 10^{-5}/^{o}C$. These two expansions are relatively close, however, the coefficient of thermal expansion for zirconia is $0.6x\ 10^{-5}/^{o}C$ (Handy & Harman of Canada, Ltd., 2008), which is about a half of that of Pd. The consequence of using zirconia with Pd is that the two materials expand at different rates, causing cracking in the Pd to occur, and leading, eventually, to the failure of the membrane.

The objective of this research was to examine the effects of support material on the characteristics of composite Pd membranes for the production of hydrogen. A porous stainless steel coated with zirconium oxide (ZrO_2) and a porous uncoated stainless steel (USS) support were used. Each of these employed a different intermetallic diffusion barrier. The membranes were prepared using an electroless plating technique that was both cost effective and capable of producing uniform dense membranes. Once made, studies were conducted to compare the hydrogen permeation characteristics as well as the long-term stability characteristics of each membrane. Some of the parameters that were investigated included the thickness of the membrane, the flux of hydrogen at varying temperatures, the selectivity achieved, and activation energy required. Once data was collected and compared, the practicality of the use of a zirconium oxide coating over an uncoated stainless steel support was analyzed.

CHAPTER 2 LITERATURE REVIEW

2.1 Membranes

Two important concepts in dealing with membranes and membrane separation are permselectivity and permeability. Permselectivity is defined as a membrane's capability of separating permeate and nonpermeate, which is also known as the retentate. The permeability of a membrane is used to identify whether a membrane has the ability of processing a large or small throughput of permeate; the higher the permeability, the higher the capacity of permeate, and vice versa. There are many processes that utilize membrane separation, including microfiltration, ultrafiltration, gas separation, reverse osmosis, dialysis, and electrodialysis, to name a few (Hsieh, 1996).

For different applications and desired permeate and retentate, different types of membranes are necessary. The two main categories of membranes are organic and inorganic. The main issues with organic membranes are that they begin to degrade once temperatures of approximately 100°C are reached and are also prone to microbial attack, which can contaminate the product. Also due to the structure of organic membranes, the pores within the membrane can close up at higher pressures, causing the permeability of the membrane to be decreased. In contrast, inorganic membranes can operate at higher temperatures and do not experience microbial attack and degradation (Hsieh, 1996). Due to better stability under harsher operating conditions, inorganic membranes can be used for a wider variety of applications than organic membranes. The major drawback to the use of inorganic membranes over organic membranes is their significantly higher material cost.

2.1.1 Metallic

The two major classes of metallic membranes include those that are dense and those that are porous. Silver porous membranes, introduced in the mid-1960s, have had quality problems with pore size and distribution. Stainless steel microporous membranes have long been used in the dairy industry and as supports for dense metallic membranes. Dense metallic membranes, on the other hand, are much less frequently used. There are several metals that are being developed for use in dense membranes; they include Pd, tantalum, vanadium and niobium. Another frequently used metal is silver, which has selectivity for oxygen (Hsieh, 1996). Pd will be used for this research due to its high selectivity and catalytic property towards hydrogen.

2.1.1.1 Palladium

Low selectivity is experienced using porous membranes for the application of hydrogen separation. This is because the separation is based on Knudsen diffusion (Mardilovich, et

al., 1998). This can be contrasted with the high selectivity achieved using dense Pd-based membranes for the use of hydrogen separation. The high degree of separation can be credited to the diffusion mechanism in a defect-free dense Pd membrane (Kikuchi, 1995).

Even though there are other metals that are permeable to hydrogen, the benefit of using Pd is its catalytic properties with hydrogen. On the Pd membrane, molecular hydrogen on the high-pressure side is adsorbed onto the surface and dissociates to become atomic hydrogen. In this form, it penetrates through the dense membrane via diffusion, and recombines on the low pressure side of the membrane to form molecular hydrogen, before desorbing. Other metals, such as vanadium, tantalum and niobium, only are able to transport diatomic hydrogen (Gryaznov, 1986). Another benefit to using Pd is that it does not oxidize as easily as the other hydrogen-permeable metals.

2.2 Membrane Preparation

There are several different methods currently available for the production of dense Pd membranes. Each method has its own advantages, but will produce membranes with varying characteristics. The goal of each technique is to produce a layer of Pd that is not only uniform, but as thin as possible. Plating methods employed can be categorized as either physical, where the membrane is applied to the support surface, or chemical, where the membrane is chemically bonded to the support. The most commonly used methods within the physical group are magnetron sputtering, high velocity oxy fuel flame sputtering, and atmospheric plasma spraying. In terms of chemical methods used for plating, the most commonly used method is electroless plating.

2.2.1 Activation and electroless plating

Electroless plating uses an autocatalytic chemical reaction to deposit Pd from the solution onto the porous supports. Porous stainless steel has been used for the support due to the advantages of having a similar thermal expansion coefficient to that of Pd and Pd-alloys, good resistance to corrosion, and increased stability through thermal changes (Dittmeyer, et al., 2001). Due to the large, non-uniform surface-pores on the stainless steel, the difficulty in depositing a defect-free thin Pd film is increased (Wang, et al., 2004).

In order to plate Pd onto the support, the surface must first be activated. This activation places Pd ion seeds on the surface of the support (Cheng & Yeung, 1999). After activation, the support is placed in a solution that contains dissolved Pd ions, EDTA, to stabilize the amine complex, and ammonia hydroxide to help stabilize and maintain the pH (Yeung, et al., 1999). Hydrazine is used as the major reducing agent and is added to cause the Pd ions to deposit out of solution onto the support, specifically onto the areas that were activated

before. The overall reaction, as presented by Mardilovich, et al. (1998), can be seen in Equation 1.

$$2Pd(NH_3)_4Cl_2 + H_2NNH_2 + 4NH_4OH \rightarrow 2Pd + N_2 + 8NH_3 + 4NH_4Cl + 4H_2O$$

or (1)

$$2Pd^{2+} + H_2NNH_2 + 4OH^- \rightarrow 2Pd^0 + N_2 + 4H_2O$$

Electroless plating is advantageous due to its low cost (Cheng & Yeung, 2001)and its ability to form a uniform layer of Pd on all edges and pores in the support (Uemiya, et al., 1991). Electroless plating has been demonstrated for use on porous stainless steel supports by several papers, including Shu, et al. (1993), Ma, et al. (2000), and Ayturk, et al (2006). It is because of these benefits that the membranes were prepared in this manner for this study.

2.2.1.1 Electroless plating under a vacuum

As plating continues, it can become more difficult to plug all the openings and create a dense membrane. Through the use of an aspirator, a vacuum was drawn on the interior of the support to aid in the plating process. The purpose of this is to pull the plating solution into any pores of the membrane that have not yet been filled.

2.2.2 Intermetallic Diffusion Barrier

Due to the high operating temperatures of the membranes, intermetallic diffusion became a significant concern (Ayturk, et al., 2006). One method that was developed by Ma, et al. (2000) was an *in situ* oxidation technique where a layer of oxides was produced on the surface of a porous sintered metal tube before it was plated (Ma, et al., 2004).

A bi-metal multi-layer (BMML) deposition technique developed by Ma, et al. (2004) and used by Ayturk, et al. (2006) has been shown to prevent intermetallic diffusion. This additional layer was coated with a top layer of Pd to produce a dense membrane. Results showed that by adding the additional BMML, the lifespan of the membrane was greatly increased. This BMML was generated by layering Ag and Pd on top of each other in sequential platings. This BMML on top of an oxide layer has been proven to successfully minimize diffusion between the metals allowing hydrogen to continue to permeate through the membrane. However, for a ceramic coated support, the BMML was unnecessary due to the nearly non-existent interactions between the ceramic and Pd. Another advantage to the BMML technique was that the addition of silver to Pd has produced an alloy that aided in preventing hydrogen embrittlement (Yepes, et al., 2006). Cheng and Yeung (1999), as well as Mardilovich, et al. (1998), found that the addition of silver improves the permeation flux of hydrogen without having major effects on selectivity.

2.3 Sieverts Law and Hydrogen Diffusion through Pd Membranes

The hydrogen flux, J, through a membrane can be described by Equation 2 through the relation of the difference of the pressure of hydrogen raised to the exponent of n, and permeance, F; or permeability, Q, and the thickness of the membrane, L. When the pressure exponent, n, is equal to 0.5, the rate limiting step of the entire process of hydrogen permeation from the high pressure side of the membrane and to the low pressure side of the support is the diffusion of hydrogen through the bulk of the Pd, which is known as Sieverts Law. Sieverts law is derived from Fick's First Law of diffusion, which states that the flux that occurs is proportional to the pressure or concentration gradient.

$$J = \frac{Q}{L}(P^n - P_o^n) = F(P^n - P_o^n) \tag{2}$$

When the pressure exponent, n, is not equal to 0.5, this indicates that the rate limiting step of the process is not the diffusion of hydrogen through the bulk of the Pd and that something else is hindering the rate of the process, which can include, but is not limited to hydrogen migration through Pd grain boundaries (Yan, et al., 1994), hindrance caused by surface processes (Collins & Way, 1993; Jayaraman & Lin, 1995), or the mass transfer resistance of the pores of the support.

The flux of hydrogen occurs from the side of the membrane where there is a high partial pressure of hydrogen to the side where there is a low partial pressure. The permeation of hydrogen through a Pd membrane involves a series of steps, which include adsorption, dissociation, diffusion, and recombination coupled with desorption. Each of these steps can be modeled with a rate equation, which can be obtained through experimentation (Ward & Dao, 1999). Mardilovich, et al. (1998) have discussed how to determine the permeability of the membrane through the use of Sieverts Law.

Analyzing Equation 2, it can be seen that by reducing the thickness of the Pd layer, the flux of hydrogen through the membrane can be increased. In addition it is also true that if the pressure difference were reduced, then the flux would also decrease. The temperature dependence of the permeability of hydrogen through Pd can be determined according to the Arrhenius relation, seen in Equation 3 (Mardilovich, et al., 1998).

$$\mathrm{Q} = \mathrm{Q_o}\exp\left[-\frac{\mathrm{E}}{\mathrm{RT}}\right] \tag{3}$$

It can be seen from Equation 3, that there is a dependence of permeability on the operating temperature of the system. Due to the presence of the temperature variable in the exponent, as temperature increases, so does permeability. The permeability is a physical

property of the material being tested and, in general, remains constant for each temperature.

Permeance, F, is the relationship between the permeability of hydrogen through the membrane to the membrane thickness (Rothenberger, et al., 2004), as seen in Equation 2. If the membrane follows Sieverts Law, the permeance can be calculated from the slope of the linear trend through the fluxes at varying the difference of the square roots of pressure for a constant temperature. Since permeability increases with temperature, permeance does as well. The meaning of permeability and the significance of this equation will be discussed further in the following section.

2.3.1 Permeability and Activation Energy

Permeability is the ability of a membrane to be permeable to a given substance. As seen previously, the permeability of a membrane can be described by Equation 3. The activation energy of a membrane can be determined by rearranging the Arrhenius equation and relating the natural log of permeance obtained from Sieverts Law data to the inverse of temperature in Kelvin. A linear plot results from the comparison of these two parameters, following the relation in Equation 4.

$$\ln(F) = \left(\frac{-E_a}{R}\right)\left(\frac{1000}{T}\right) + \ln(F_o) \tag{4}$$

The slope of the linear trend can be used to determine the activation energy using Equation 5, where R is the universal gas constant.

$$E_a = (slope)(R) \tag{5}$$

Ayturk (2007) collected activation energy values for a Pd free-standing foil from various sources and found them to range between 13.5 kJ/mol and 18.6 kJ/mol, with an average value of 15.63 kJ/mol.

2.4 Membrane Characteristics

Depending on the individual parameters associated with a membrane, the characteristics achieved can be very different. Some of the important factors that can contribute to varying characteristics are the selectivity of the membrane, plating thickness, whether or not an intermetallic diffusion barrier is used, as well as the type of barrier, plating solution composition, and support type.

2.4.1 Ideal Selectivity

The ideal selectivity of a membrane is determined by its flux characteristics and is the relationship between the hydrogen flux achieved and the flux of the inert gas that is used,

which was helium in this study. Equation 6 can be used for the calculation of ideal selectivity, $\alpha_{H2/He}$, and is used for fluxes obtained at similar temperatures and differential pressures.

$$\alpha_{H_2/He} = \frac{J_{H_2}}{J_{He}} \tag{6}$$

If a dense, defect-free membrane was produced, it would be impermeable to helium. Therefore, the selectivity would increase to infinity. Therefore, the goal was to achieve as high of a selectivity as possible in order to obtain a high purity hydrogen product.

2.4.2 Free-Standing Palladium Films

A comparison of the plated membranes can be made to their free-standing film counterparts. In doing so, the maximum attainable permeability can be related to the actual permeability obtained for each membrane. By comparing permeabilities, both membranes can be compared on a similar scale since permeability is a thickness-independent characteristic. Using Equation 3, the permeability can be calculated, where Q_o has a value of 6322.7 $m^3 \cdot \mu m/m^2 \cdot h \cdot atm^{0.5}$ and E_a is equal to 15630 kJ/mol. The pre-exponential factor, Q_o, and the activation energy, E_a, were determined through a linear regression of previous data conducted on free standing thin Pd films by Ayturk (2007). From these data, a percentage of the maximum achievable permeability for each of the membranes at each of the testing temperatures can be determined.

Using the free-standing film permeability for each temperature, Sieverts Law, as seen in Equation 2, can be used to calculate the pressure at the interface of the Pd layer and the porous support. The measured values are the shell-side pressure, which was set during testing, the flux measured during testing, as well as the membrane thickness. The free-standing film permeability can be determined based upon the measured values obtained during testing. The only unknown is P_x, or membrane/support interface pressure. It is possible to calculate P_x by understanding that the flux of hydrogen through the Pd membrane ($J_{H2\text{-}Pd}$) is the same as the flux through the support ($J_{H2\text{-}Support}$) at steady state. A schematic of the pressure P_x can be seen in Figure 1, as presented by Ayturk (2007).

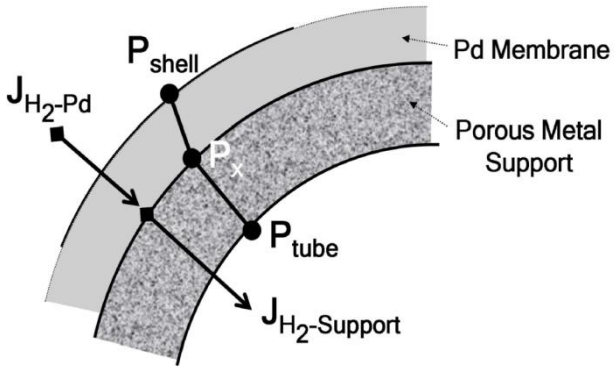

Figure 1: Schematic for the H_2 flux through a Pd membrane coated on a porous support

In determining the pressure drop experienced individually by both the membrane and the support, a fraction of the total mass transfer resistance can be calculated for each of the two parts. Results from these calculations are able to reveal whether the resistance across the system is mainly due to the membrane or to the support characteristics.

CHAPTER 3 EXPERIMENTAL

The focus of our study was to prepare two dense Pd membranes, plated onto supports obtained from Pall Corporation. The first support was made of porous uncoated stainless steel (USS). Prior to plating an intermetallic diffusion barrier oxide layer was generated. The second membrane was a porous stainless steel support that had an additional layer of zirconium oxide (ZrO_2) sintered on the surface of the stainless steel by the manufacturer (Wang, et al., 2004). This zirconium oxide layer acted as the intermetallic diffusion barrier for the second membrane in our study.

Both membranes were produced using an electroless plating method. The Pd/silver barrier was used to prevent intermetallic diffusion. The addition of silver (Ag) to palladium (Pd) lowers the overall cost of the membrane and also prolongs the lifespan of the membrane by preventing the intermetallic diffusion between the porous stainless steel and the Pd. The thickness of the membrane could be calculated using the gravimetric method, as seen in Appendix I, where the weight of the plating deposited on the support and the density of the plated substance can be used to find the average thickness of the plating achieved (Ma, et al., 2004).

Through characterization studies, the effects of the ceramic oxide layer, in substitution of the metallic oxide layer, were evaluated. Membrane characteristics were the main focus of the conducted study. The membrane supported by porous stainless steel (USS/Pd) was compared to the membrane plated on the zirconium oxide coated support (ZrO_2/Pd) in order to investigate how the characteristics of each membrane differed due to the extra ceramic barrier layer of zirconium oxide on one of the membranes. It was expected that the ceramic oxide layer would yield a higher flux of product and a longer lifespan due to the lack of intermetallic diffusion that would occur between the support and the membrane. What was uncertain in this study was how the membrane with zirconium oxide coating would behave at elevated temperatures, where the coefficients of thermal expansion would begin to play a critical role in membrane integrity and functionality.

CHAPTER 4 METHODOLOGY

4.1 Support Preparation

4.1.1 Helium Leak Testing

Testing of the support was done prior to any treatment or plating to determine the flux of helium through the support, which allowed the initial fluxes of the two supports to be compared to each other. To conduct the testing, the support was connected to a system where He was flowed through the shell-side of the support with the shell-side outlet plugged. Therefore, the helium was forced to permeate through the porous support tube and enabled the calculation of the flux of the leak for each of the supports.

The pressure of the helium feed set to be approximately 1.25 bar, and the flux for the stainless steel support was measured on the wet test meter by recording the time necessary for $9x10^{-3}$ m^3 of helium to pass through. The pressure was then increased at 0.25 bar intervals until either a maximum flowrate of $5x10^{-4}$ m^3/s or maximum pressure of 3.5 bar was achieved. This process was then repeated for the zirconium oxide coated support. The graph of the flux of helium against the differential pressure gave a linear plot. The slope of this linear trend represented the permeance of the support. Therefore, as the shell-side pressure was increased, the helium flux through the support increased proportionally.

This procedure was repeated as plating continued until the membranes were gas tight. As the flow of helium decreased due to a denser Pd layer, data collection switched from the wet test meter to a digital flow meter to a bubble flow meter for more accurate measurements.

4.1.2 Cleaning

It was necessary to clean the supports prior to any treatment or plating to ensure that there were no contaminants present. The supports were cleaned with successive dipping in the cleaning solutions Na_3PO_4, Na_2CO_3, and NaOH and then washing in an ultrasonic bath for 30 minutes. The detailed procedure can be seen in Appendix II.

4.1.3 Support Oxidation

Since there was no intermetallic diffusion barrier present on the porous uncoated stainless steel support, one had to be produced. To do this, the support was placed in an oven at $500^{o}C$ for 12 hours in order to oxidize the surface of the stainless steel. This aided in the prevention of intermetallic diffusion between the stainless steel and the Pd once it had been plated. A detailed procedure can be seen in Appendix II.

4.2 Palladium Deposition

A series of steps were taken in order to deposit Pd onto the surface of each of the supports. Activation steps had to be performed in order to seed Pd ions on the surface, followed by the actual plating process. The activation utilized three solutions: $SnCl_2$, PdCl and 0.1M HCl, in order to deposit Pd ions onto the surface. The actual plating process consisted of the use $Pd(NH_3)_4Cl_2$ as the plating solution and N_2H_4 as the major reducing agent in a 60°C bath. Detailed steps of the two processes can be seen in Appendix II.

4.3 Hydrogen Testing

Hydrogen testing was performed on each of the membranes in order to determine their characteristics. The membranes were placed into the reactor testing units seen in Figure 2, as presented by Mardilovich, et al. (1998).

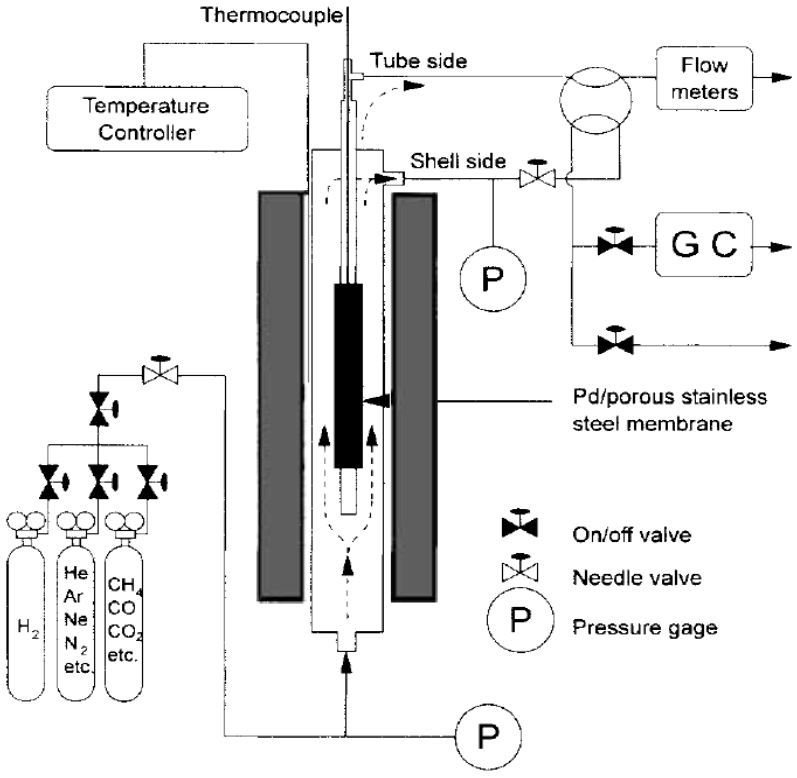

Figure 2: Hydrogen testing reactor set up

The hydrogen feed entered at the bottom of the reactor and permeated through the membrane from the high pressure shell-side to the low pressure tube-side. Each membrane was heated from room temperature to an initial testing temperature of 300°C at

a rate of 0.5°C/min under helium with a differential pressure of 1.0 bar between the shell- and tube-side pressures. He leak testing was performed at a differential pressure of 3 bar at each of the studied temperatures. After the testing was completed, the membrane was then subjected to hydrogen testing. Once the hydrogen flux stabilized, testing was done to obtain the flux at differential pressures in the range of 0.5 bar to 4 bar, increasing the pressure in increments of approximately 0.5 bar. After hydrogen testing at a given temperature was completed, the membrane was then run under helium to again take the leak data. This testing was performed at 350°C and 400°C, heating at a ramp rate of 1.0°C/min. The temperature was then decreased, and tests were redone at 350°C and 300°C to determine if the characteristics of each membrane had changed due to the membrane being exposed to higher operating temperatures. After testing had been completed, each membrane was cooled to room temperature at a rate of 0.5°C/min and then was removed from the testing units.

CHAPTER 5 RESULTS AND DISCUSSION

5.1 Membrane Preparation

5.1.1 Plating Sequence

The goal of the plating was to obtain a defect-free dense membrane on the surface of each of the supports. A full plating history can be seen in Appendices III and IV for a detailed description of what occurred during each round of plating for each of the two membranes.

5.1.2 Helium Flux Testing and Final Membrane Characteristics

Helium flux testing was done in between plating steps for each membrane so as to monitor how each step affected the overall denseness of the membrane. As the membrane became more dense, the helium flux through the membrane decreased. Figure 3 shows the progression of each membrane during the preparation and plating steps. The diamonds represent the uncoated stainless steel support and the squares represent the zirconium oxide coated support. Each linear regression represents one stage of the plating process: the highest flux achieved by each membrane was the initial flux when the supports were obtained and each thereafter was a plating round.

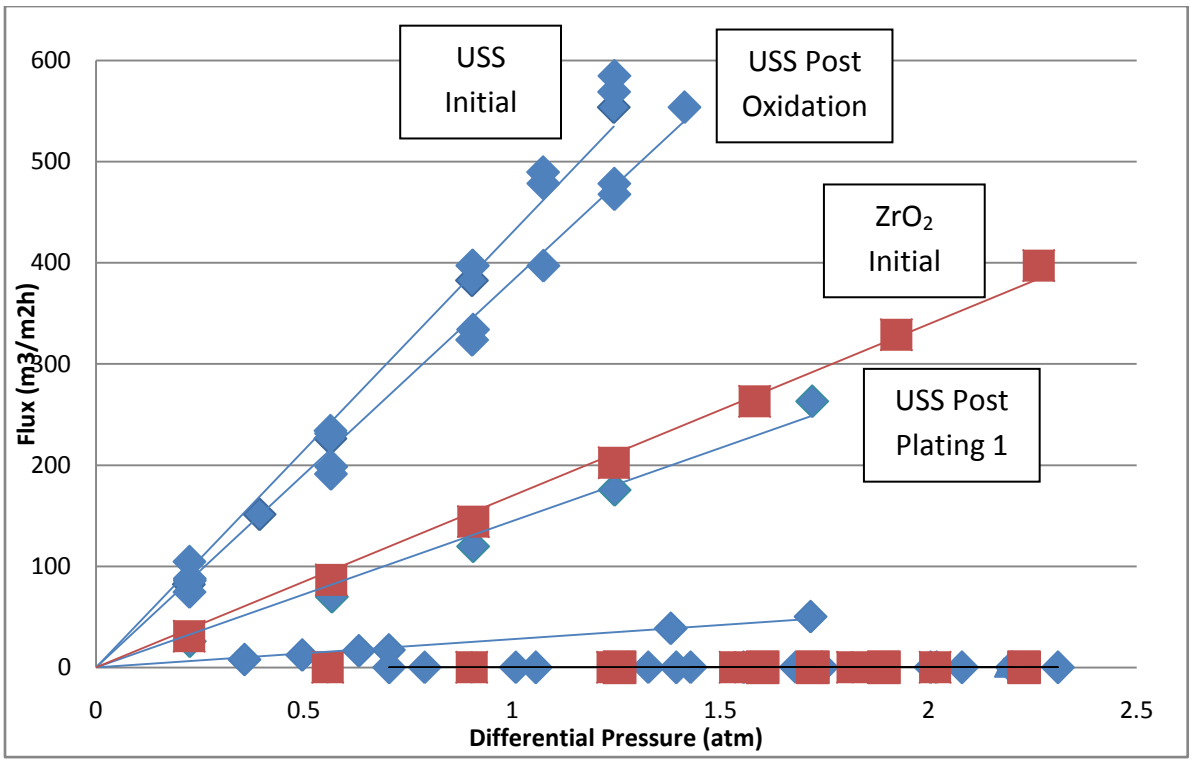

Figure 3: Helium leak data during membrane preparation

After four rounds of plating, the membrane plated on top of the zirconium oxide coated support (ZrO_2/Pd membrane) became dense. This was determined when the membrane was tested at room temperature for leaks with helium (He) and no flux was detected at a differential pressure of 2.5 bar. The ZrO_2/Pd membrane had a total thickness of 6.9 µm. After eight rounds of plating the USS (USS/Pd membrane) was considered to be dense. The larger number of plating rounds was due in part to pinhole-sized defects that formed near the welding joints. Due to these complications during the plating process, a final flux of He of 0.11 SCCM at a differential pressure of approximately 2.5 bar was still present after the final plating. The final thickness of the membrane plated onto the USS support was 54.1 µm. Calculations for thickness can be found in Appendix III Plating history and helium flux data for USS membrane**.**

The large discrepancy between the thicknesses of the two membranes was expected. By coating the porous stainless steel support with zirconium oxide, the pore sizes are further reduced, which caused the support to have an initial helium flux that was roughly the same as the flux of the USS support after one round of plating, as seen previously in Figure 3. The reduced pore size also enabled the ZrO_2/Pd membrane to fill open pores more quickly. After the second round of plating, the ZrO_2/Pd membrane had a maximum He flux of 0.2 m^3/m^2h measured at a differential pressure of 2.5 bar, while it took the USS/Pd membrane a total of six plating rounds to obtain a He flux that low at the same differential pressure. Figure 4 shows schematically the varying plating microstructures on the two different supports.

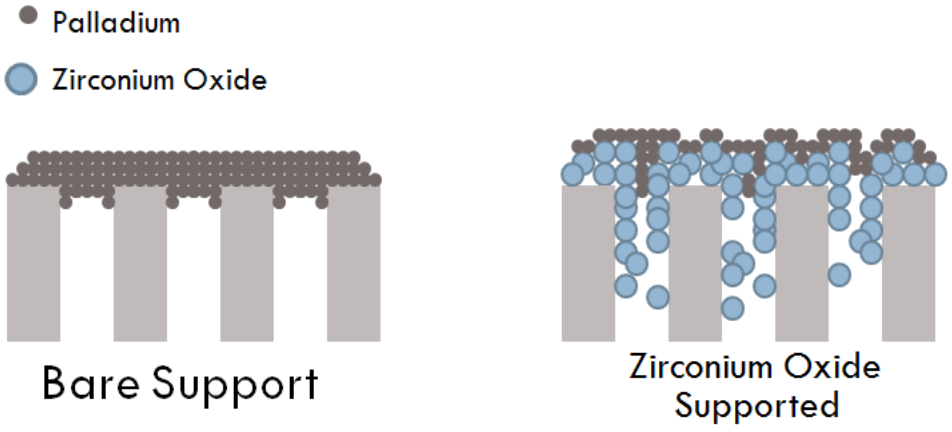

Figure 4: Schematic of Pd plated on uncoated stainless steel versus a zirconium oxide coated support

The final values for the various physical characteristics of each of the membranes can be seen in Table 1.

Table 1: Physical characteristics of the membranes after plating

	Uncoated Stainless Steel Supported Membrane	ZrO_2 Coated S/S Supported Membrane
Initial Weight (g)	138.43	140.00
Final Weight (g)	139.84	140.17
Surface Area (cm^2)	15.4	15.4
Plating Thickness (µm)	54.1	6.9
Final He Leak (SCCM)	0.111	0
Total Plating Rounds	3 x Regular	3 x Regular
	5 x Vacuum	1 x Vacuum

5.2 Hydrogen Permeation Tests

5.2.1 Sieverts Law Plots and Hydrogen Flux Data

The hydrogen flux of the two membranes could be represented by Figure 5, which represents the data from ZrO_2/Pd membrane, and Figure 6, which represents the data from the USS/Pd membrane.

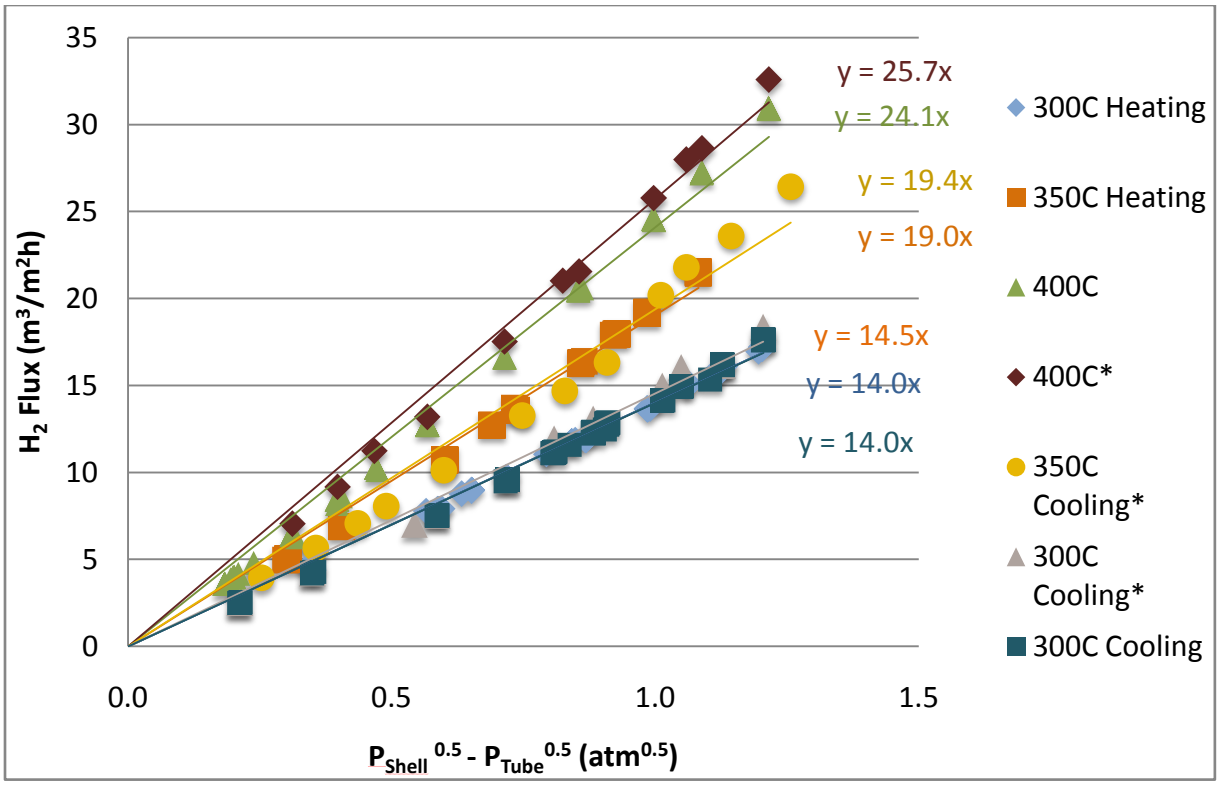

Figure 5: Sieverts plot for membrane plated on zirconium oxide coated support

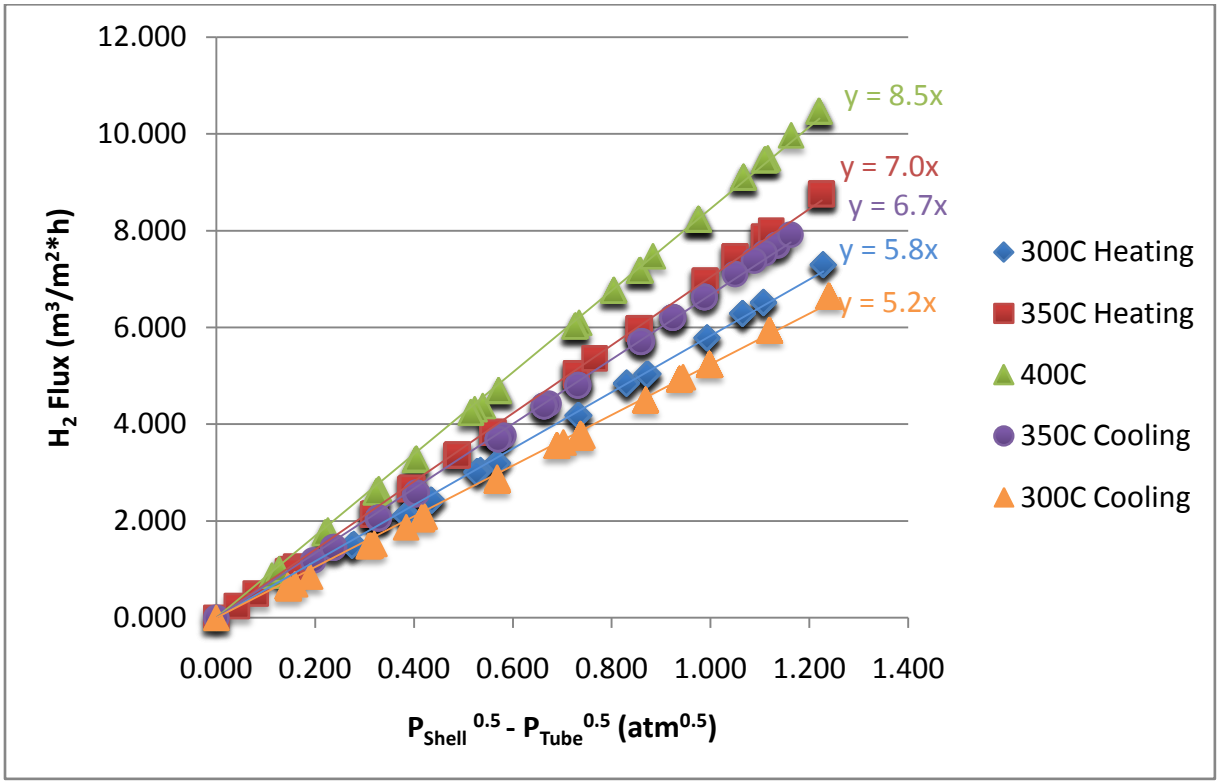

Figure 6: Sieverts plot for membrane plated on USS support

The maximum flux attained by the ZrO_2/Pd membrane, as seen in Figure 5, was approximately 32.5 $m^3/m^2 \cdot h$ at 400°C at a differential pressure of 4 bar. This is much higher than the maximum flux of the USS/Pd membrane seen in Figure 6, which attained a maximum flux of approximately 7.5 $m^3/m^2 \cdot h$ at 400°C at a similar differential pressure. The higher flux of the ZrO_2/Pd membrane can be explained by Equation 2. Q, the permeability, is a constant value for Pd films of any thickness and at 400°C, and the maximum differential pressures for both membranes were the same. Therefore, the distinguishing factor that causes a higher flux from the ZrO_2/Pd membrane was thickness.

5.3 Free Standing Film Calculations

While the ZrO_2/Pd membrane was able to reach a much higher permeability than the USS/Pd membrane, it was not able to reach as much of its expected permeability for its thickness. Table 2 shows the measured permeability versus the free standing film permeability for each temperature.

Table 2: Comparison of theoretical and experimental permeability data

Support	Temperature	Permeability Measured	Free Standing Permeability	% of Free Standing
	˚C	$m^3 \cdot \mu m/m^2 \cdot h \cdot atm^{0.5}$	$m^3 \cdot \mu m/m^2 \cdot h \cdot atm^{0.5}$	
USS	300 Heating	223.64	237.70	94.1%
	300 Cooling	201.06	237.70	84.6%
	350 Heating	256.27	309.30	82.9%
	350 Cooling	269.96	309.30	87.3%
	400	324.06	387.03	83.7%
ZrO_2	300 Heating	105.65	237.70	44.4%
	300 Cooling	91.31	237.70	38.4%
	350 Heating	117.26	309.30	37.9%
	350 Cooling	125.36	309.30	40.5%
	400	172.07	387.03	44.5%

Permeability is a thickness-independent value, allowing the two membranes to be compared on an equal scale. While the USS/Pd membrane was able to obtain roughly 85% of the theoretical flux for a free standing Pd film, the ZrO_2/Pd membrane was only able to reach 40% on average. This was due to the nature of the ZrO_2 coating. The further reduction of the pores caused a higher percentage of the pressure drop to occur across the porous support, and therefore a smaller pressure drop across the actual membrane. The pressure drop across the membrane layer was calculated using the difference of the square

roots of pressure across the membrane. According to Equation 2, a reduction of pressure drop across the membrane directly reduced the flux. The proportion of resistance that comes from each layer was calculated, and the fraction of the total resistance across each system that was taken up by the support can be seen in Figure 7. The USS support offered little resistance to mass transfer, while the ZrO_2 support presented significant resistance to mass transfer across the layers membrane and support layers.

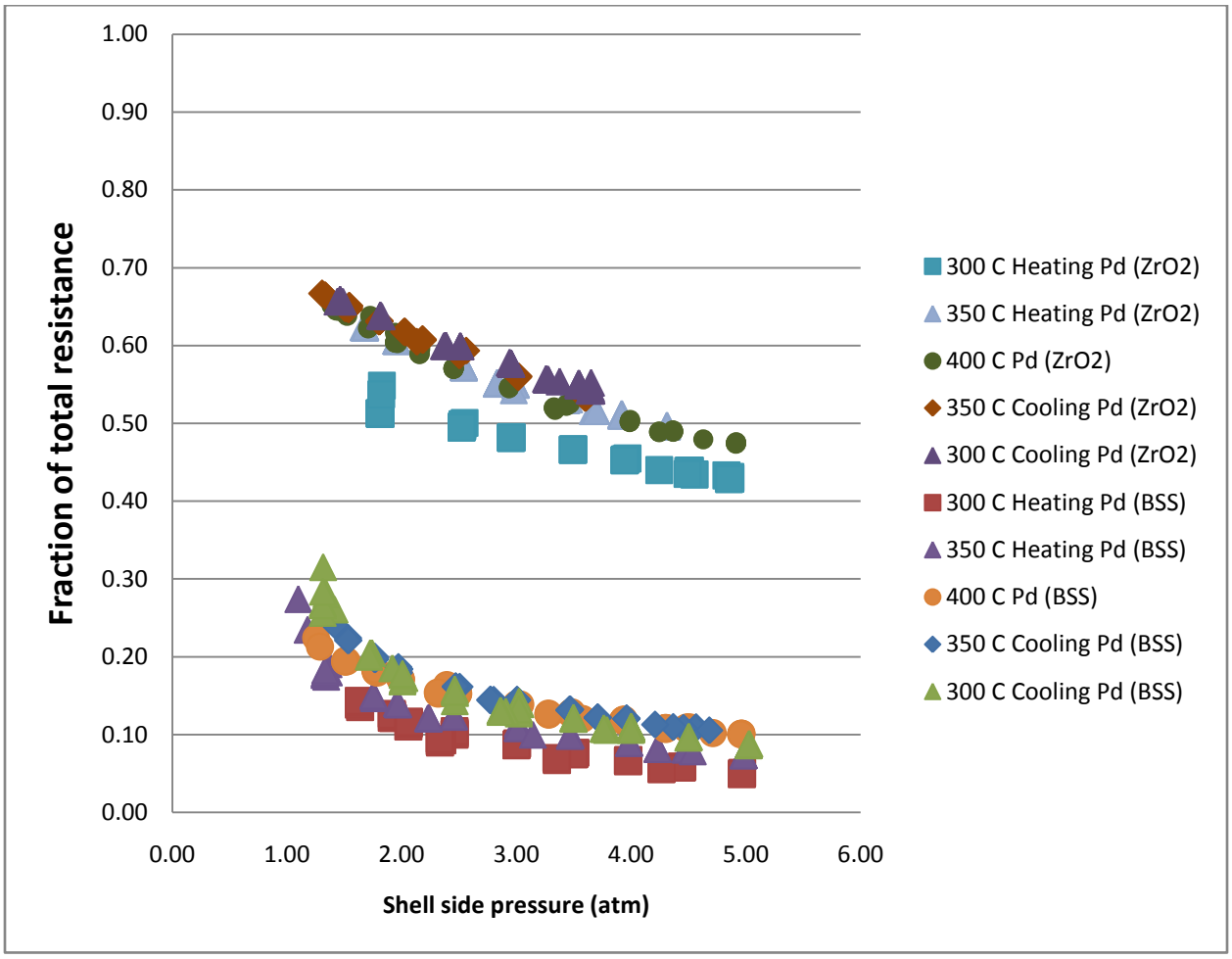

Figure 7: Comparison of the fraction of the total resistance experienced by the support

The USS support caused 5% to 30% of the total pressure drop, compared to the ZrO_2, which caused 43% to 67% of the total pressure drop across the layers. It is important to understand what effect the support layer of each system played in terms of the total pressure drop across the layers of the membrane and support. If the larger portion of the pressure drop was experienced in the Pd layer, then most of the resistance through the system was experienced by the bulk diffusion of the hydrogen through the Pd. On the other hand, if a significant portion of the pressure drop across the both layers was experienced passing through the support, then the resistance of the support was large enough to play a

role in the total mass transfer of hydrogen through the layers of the membrane and the support. Therefore, the resistance of the support must be taken into account during calculations of pressure drop.

5.3.1.1 Hydrogen Flux Stability

In the USS/Pd membrane, the flux attained when the membrane was cooled was lower than that attained when heating. It was expected that as the membrane was heated, leaks would form, which in turn would increase the flux as time increased. The reason the USS/Pd membrane did not exhibit this can be explained by the thickness. The large thickness allowed the membrane to be able to withstand the formation of leaks. However, the reduction of flux was likely due to some intermetallic diffusion that might have occurred between the support and the membrane. While steps were made to prevent this from occurring, there was still a possibility that it did occur. Further spectroscopy analysis would be needed to determine this for certain. The ZrO_2/Pd membrane followed the expected model of having a higher flux when cooling compared to heating. Table 3 shows that as testing progressed, the selectivity of the ZrO_2/Pd membrane decreased, which will be discussed in the next section.

5.3.2 Helium Leak and Selectivity

The ideal selectivity, given by Equation 4, was calculated at a differential pressure of 3 bar, before and after each hydrogen flux testing. The results can be seen in Table 3.

Table 3: Selectivities of membranes

Temperature (°C)		USS Selectivity	ZrO_2 Selectivity
300 Heating	Before	∞	1354
	After	4077	1142
350 Heating	Before	4764	1101
	After	4491	920
400	Before	1624	1294
	After	3024	1757
350 Cooling	Before	1078	1331
	After	2783	1293
300 Cooling	Before	1091	908
	After	1035	932

Due to the thickness of the USS/Pd membrane, it exhibited a much higher selectivity towards hydrogen during initial testing, because at the elevated temperature at which testing occurred, the helium leak through the USS/Pd membrane was undetectable by means of measurement available. A reason this could have occurred could be attributed to the type of diffusion that dominated in the support pores, which was Knudsen. The flux equation that involves the Knudsen diffusion coefficient (D_K) can be seen in Equation 7, where flux is inversely proportional to temperature.

$$J = \frac{D_K}{LRT}(P_1 - P_2) \tag{7}$$

The ZrO_2/Pd membrane on the other hand, while starting with no measureable He leak at room temperature, formed a leak while heating. This is explained by the difference between the thermal expansion coefficients of the ceramic and Pd layers, which may have caused a leak.

5.3.3 Activation Energy

The activation energy for each of the two membranes was calculated from the Arrhenius relation seen in Equation 5. By plotting the natural log of permeance versus 1000 multiplied by the inverse of temperature in Kevin, linear relations were developed as seen in Figure 8.

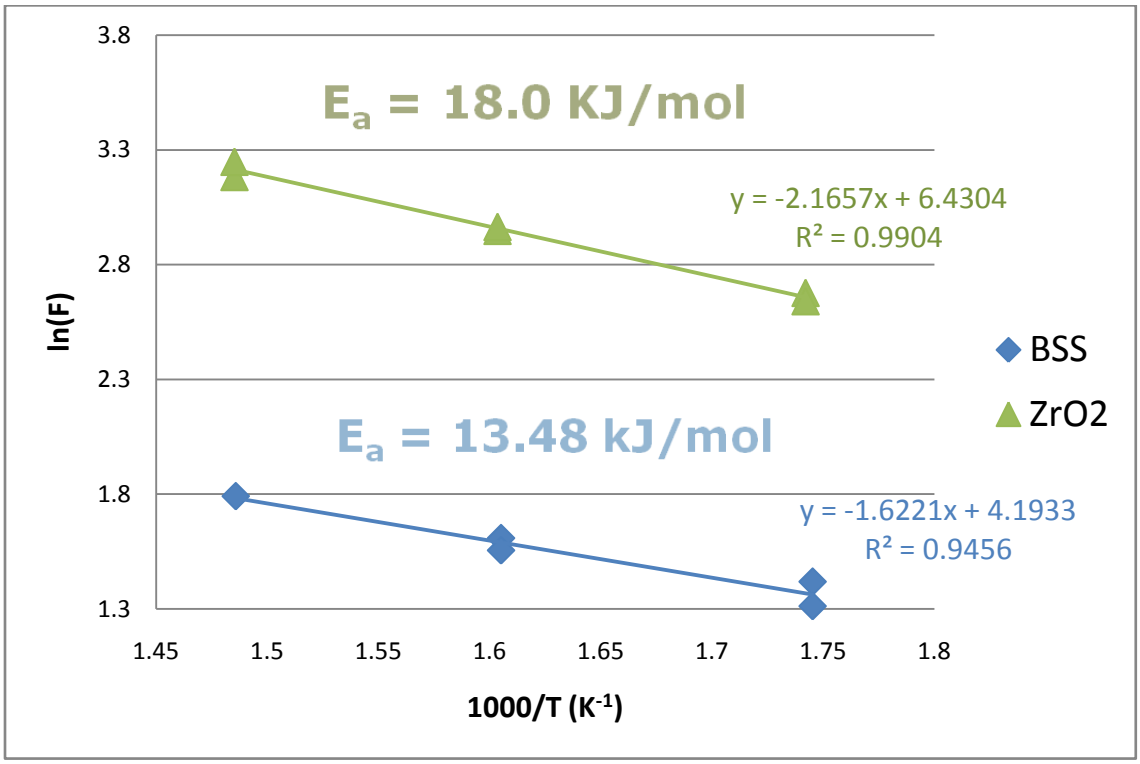

Figure 8: Comparison of the activation energies experienced by membrane plated on the USS support and that plated on the zirconium oxide coated support

The slope of the line plotted gives the negative activation energy, E_a, divided by R, the universal gas constant. Therefore, multiplying the slope by the gas constant, the activation energies for each of the membranes were obtained. The calculated activation energies for the USS/Pd membrane and the ZrO_2/Pd membrane are comparable to others that were previously reported: between 13.5 kJ/mol and 18.6 kJ/mol (Ayturk, 2007).

CHAPTER 6 Conclusions

Through the research that was conducted, some conclusions were drawn:

- The ZrO_2 coating on the stainless steel allowed for a thinner membrane
- The ZrO_2/Pd has a higher flux than that of the USS membrane at similar pressures and temperatures.
- The USS membrane required a thicker coating of Pd
- The USS coated membrane achieved a much higher percentage of its free-standing foil flux as compared to the ZrO_2/Pd membrane.
- While plating a thinner membrane on the ZrO_2 would not allow for greater flux due to the pressure drop of the support, reducing the thickness of the membrane on the USS would be able to yield a higher flux.
- Through the use of the Arrhenius equation, the activation energy for the ZrO_2 coated membrane was found to be higher than that of the USS membrane.

CHAPTER 7 Recommendations for Future Studies

If time had permitted, additional studies could have also been conducted. Some thoughts on this are that the membrane's operating temperature could have been incrementally increased to much higher temperatures in order to observe its changing behavior. Some characteristics that would have been observed are the interaction of the coefficients of thermal expansion, the effects on flux and permeance, as well as the integrity of the membrane during operation at these temperatures.

It may have also been possible to leave the membrane for longer periods of time at each temperature, or at least for a prolonged period when operating at one temperature, in order to observe the stability with time to perform durability tests. It would have also been possible to plate additional membranes while altering some of the techniques to produce slightly varied results, such as more silver layers to form a thicker BMML, or no silver at all to observe the role that intermetallic diffusion plays in the resulting flux of hydrogen through the membrane. It also may have been possible to produce additional membranes on porous stainless steel supports where the pores of the supports had been altered in order to make them smaller. This would have allowed a thinner membrane to be plated and increased the flux of the unit if all other parameters remained the same.

From these tests, microscopy studies could have been performed in order to fully analyze the role of intermetallic diffusion in the permeation process, as well as the thickness of the membrane and how it varied along the surface of the support.

NOMENCLATURE

E	Activation energy (kJ/mol)
F	Permeance ($m^3/m^2 \cdot h \cdot atm^n$)
J	Rate of hydrogen permeation or hydrogen flux ($mol/m^2 \cdot s$ or $m^3/m^2 \cdot h$)
L	Thickness of Pd layer (μm)
P	Pressure (bar or atm)
Q	Permeability($m^3 \cdot \mu m/m^2 \cdot h \cdot atm^{0.5}$)
Q_o	Pre-exponential form factor ($m^3 \cdot \mu m/m^2 \cdot h \cdot atm^{0.5}$)
R	Gas constant (J/mol·K)
T	Absolute temperature (K)
$\alpha_{H2/He}$	Membrane selectivity of hydrogen to helium

LITERATURE CITED

Adris, A. M., Li, C. J., & Grace, J. R. (1997). The fluidized-bed membrane reactor for steam methane reforming: model verification and parametric study. *Chem. Eng. Sci. , 52*, 1609.

Adris, A. M., Pruden, B. B., Lim, C. J., & Grace, J. R. (1996). On the reported attempts to radically improve the performance of the steam methane reforming reactor. *Can. J. Chem. Engng. , 74*, 186.

Ayturk, M. E. (2007). *Synthesis, Annealing Strategies and in-situ Characterization of Thermally Stable Composite Thin Pd/Ag Alloy Membranes for H2 Separation.* PhD Thesis, Worcester Polytechnic Institute, Chemical Engineering.

Ayturk, M. E., Engwall, E. E., & Ma, Y. H. (2007). Microstructure Analysis of the Intermetallic Diffusion-Induced Alloy Phases in Composite Pd/Ag/Porous Stainless Steel Membranes. *Ind. Eng. Chem. Res.* (46), 3295.

Ayturk, M. E., Mardilovich, I. P., Engwall, E. E., & Ma, Y. H. (2006). Synthesis of composite Pd-porous stainless steel (PSS) membranes with a Pd/Ag intermetallic diffusion barrier. *J. Membr. Sci. , 285*, 285-294.

Balachandran, U., Dusek, J., Mieville, R., Poeppel, R., Kleefisch, M., Pei, S., et al. (1995). Dense ceramic membranes for partial oxidation of methane to syngas. *Appl. Catal. A: Gen. , 133*, 19.

Cheng, Y. S., & Yeung, K. L. (2001). Effects of electroless plating chemistry on the synthesis of palladium membranes. *J. Membr. Sci. , 182*, 195.

Cheng, Y., & Yeung, K. (1999). Palladium-silver composite membranes by electroless plating technique. *J. Membr. Sci , 158*, 127.

Collins, J. P., & Way, J. D. (1993). Preparation and characterization of a composite palladium-ceramic membrane. *Ind. Eng. Chem. Res. , 32* (12), 3006-3013.

Dittmeyer, R., Hölleina, V., & Daub, K. (2001). Membrane reactors for hydrogenation and dehydrogenation processes based on supported palladium. *J. Mol. Catal. A , 173*, 135.

Elert, G. (2008). *Thermal Expamsion*. Retrieved Dec 3, 2008, from The Physics Hypertextbook: http://hypertextbook.com/physics/thermal/expansion/

Gryaznov, V. M. (1986). Hydrogen Permeable Palladium Membrane Catalysts: An Aid to the Efficient Production of Ultra Pure Chemicals and Pharmaceuticals. *Platinum Metals Rev. , 30* (2), 68-72.

Handy & Harman of Canada, Ltd. (2008). *The Brazing Book Online*. Retrieved Dec 06, 2008, from http://www.handyharmancanada.com/TheBrazingBook/comparis.htm

Hsieh, H. P. (1996). *Inorganic Membranes for Separation and Reaction.* New York: Elsevier.

Hunter, J. B. (1963). Ultrapure Hydrogen By Diffusion Through Palladium Alloys. *Symposium on the Production of Hydrogen Petroleum Division, The American Chemical Society Meeting.* New York: ACS.

Iulianelli, A., Longo, T., & Basile, A. (2008). Methanol steam reforming in a dense Pd-Ag membrane reactor: The pressure and WHSV effects on CO-free H2 production. *J. Membr. Sci.* (323), 235.

Jayaraman, V., & Lin, Y. S. (1995). Synthesis and hydrogen permeation properties of ultrathin palladium-silver alloy membranes. *J. Membr. Sci. , 104*, 251-262.

Kikuchi, E. (1995). Palladium/ceramic membranes for selective hydrogen permeation and their application to membrane reactor. *Catal. Today* (25), 333.

Lin, Y. S. (2001). Microporous and dense inorganic membranes: current status and prospective. *Separation and Purification Technology , 25* (1-3), 39-55.

Ma, Y. H., Akis, B. C., Ayturk, M. E., Guazzone, F., Engwall, E. E., & Mardilovich, I. P. (2004). Characterization of Intermetallic Diffusion Barrier and Alloy Formation for Pd/Cu and Pd/Ag Porous Stainless Steel Composite Membranes. *Ind. Eng. Chem. Res. , 43* (12), 2936-2945.

Ma, Y. H., Mardilovich, I. P., & Engwall, E. E. (2004). *Patent No. Application US2004.0237779 A1.* U.S. Provisional.

Ma, Y. H., Mardilovich, P. P., & She, Y. (2000). *Patent No. 6,152,987.* U.S.

Mardilovich, P., She, Y., & Ma, Y. (1998). Defect-Free Palladium Membranes on Porous Stainless-Steel Support. *AiChE Journal , 44* (2), 310-322.

Perry, R. H., Green, D. W., & Maloney, J. O. (Eds.). (1997). *Perry's Chemical Engineers Handbook* (7th Ed. ed.). New York: McGraw-Hill.

Richerson, D. W. (2006). *Modern Ceramic Engineering: Peroperties, Processing and Use in Design* (3rd ed.). Boca Raton, FL: CRC Press and Taylor & Francis.

Rothenberger, K. S., Cugini, A. V., Howard, B. H., Killmeyer, R. P., Ciocco, M. V., Morreale, B. D., et al. (2004). High pressure hydrogen permeance of porous stainless steel coated with a thin palladium film via electroless plating. *J. Membr. Sci. , 244* (1-2), 55-68.

Roy, S., Pruden, B. B., Adris, A. M., Grace, J. R., & Lim, C. J. (1999). Fluidized-bed steam methane reforming with oxygen input. *Chem. Eng. Sci. , 54*, 2095.

Shu, J., Grandjean, B., Ghali, E., & Kaliaguine, S. (1993). Simultaneous deposition of Pd and Ag on porous stainless steel by electroless plating. *J. Membr. Sci. , 77*, 181.

Sterlitech Corporation. (2008). *Silver Membrane Filter*. Retrieved December 03, 2008, from http://www.sterlitech.com/441463/products/Silver-Membrane-Filter.html

Uemiya, S., Matsuda, T., & Kikuchi, E. (1991). Hydrogen permeable palladium-silver alloy membrane supported on porous ceramics. *J. Membr. Sci. , 56*, 315.

Wang, D., Tong, J., Xu, H., & Mastumura, Y. (2004). Preparation of palladium membrane over porous stainless steel tube modified with zirconium oxide. *Catal. Today* (93-95), 689.

Ward, T. L., & Dao, T. (1999). Model of hydrogen permeation behavior in palladium membranes. *J. Membr. Sci. , 153*, 211.

Yan, S., Maeda, H., Kusakabe, K., & Morooka, S. (1994). Thin Palladium Membrane Formed in Support Pores by Metal-Organic Chemical Vapor Deposition Method and Application to Hydrogen Separation. *Ind. Eng. Chem. Res. , 33* (3), 616-622.

Yepes, D., Cornaglia, L. M., Irusta, S., & Lombardo, E. A. (2006). Different oxides used as diffusion barriers in composite hydrogen permeable membranes. *J. Membr. Sci. , 274*, 92.

Yeung, K. L., Christiansen, S. C., & Varma, A. (1999). Palladium composite membranes by electroless plating technique: Relationships between plating kinetics, film microstructure and membrane performance. *J. Membr. Sci. , 159* (1-2), 107.

Appendix I Sample Calculations

Flux Calculation

Using the uncoated stainless steel membrane after first mechanical treatment (17 Nov 09) as an example:

Data

- Pressure: 18 psig
- Time: 3:21 (min:sec)
- Volume: 9L

Convert

Pressure from psig to atm

$$18.0\ psi - 14.7\ psi(atm\ pressure) = 3.30\ psi$$

$$3.3\ psi * 0.068 \frac{atm}{psi} = 0.224\ atm$$

Time to hours

$$3{:}21 = 3\ min\ 21\ sec = 201\ sec$$

$$201\ sec * \frac{1\ hr}{3600\ sec} = 0.056\ hr$$

Volume from L to m^3

$$9\ L * \frac{m^3}{1000L} = 0.009 m^3$$

Find surface area

- Length: 0.049 m
- Diameter: 0.01 m

$$\pi * D * L = SurfaceArea$$

$$3.14 * 0.049 * 0.01 = 0.0015 m^2$$

Flux is the volume that passes through a given area in a certain time period (Units $\frac{m^3}{m^2 * hr}$)

From above

- Volume: 0.009 m^3
- Surface Area: 0.0015 m^2
- Time: 0.056 hr

$$Flux = \frac{0.009 m^3}{0.0015 m^3 * 0.056 hr} = 104.71 \frac{m^3}{m^2 \cdot hr}$$

Plating thickness

Using the uncoated stainless steel membrane after the first plating round as an example:

Data

- Initial Weight: 138.43 g
- Weight After Plating: 138.77 g
- Plating Length: 0.069 m
- Diameter: 0.01 m

- Density of Pd: 12.01 g/cm^3

Surface Area

$$\pi * D * L = SurfaceArea$$
$$3.14 * 0.069 * 0.01 = 0.00217m^2 = 21.7cm^2$$

Plated Weight

$$138.77g - 138.43g = 0.34g$$

Plating Thickness

$$\frac{Platedweight\ (g)}{SurfaceArea(cm^2)} x \frac{1}{DensityofPd\ (^{g}/_{cm^3})}$$

$$\frac{0.34g}{21.7cm^2} x \frac{1}{12.01\ ^{g}/_{cm^3}} = 0.001305\ cm$$

Convert to µm

$$0.001305cmx \frac{10{,}000\mu m}{cm} = 13.05\mu m$$

Appendix II Experimental Procedures

AII.1 Support Preparation

AII.1.1 Cleaning

1. Pour 250 mL of water into a 1 liter flask.
2. Add 45 g Na_3PO_4; shake until dissolved.
3. Add 65 g of Na_2CO_3; shake until dissolved.
4. Add 45 g of NaOH; shake until dissolved.
5. Add ~5 mL of detergent.
6. Dilute solution up to 1 liter with DI water.
7. Place supports in graduated cylinders.
8. Fill cylinders with cleaning solution.
9. Place cylinders into heated ultrasonic water bath for 30 min.
10. Remove; wash with tap water for 1 hr.
11. Wash with DI water 10 times.
12. Place into graduated cylinder, fill with DI water.
13. Place cylinders into ultrasonic bath for 10 min.
14. Rinse support, change DI water and place back into bath for 5 min.
15. Repeat step 11 while checking pH. Repeat rinsing/ultrasonic bath until pH is neutral.
16. Wash supports with isopropanol (IPA).
17. Place supports into ultrasonic bath with IPA.
18. Dry at 120^{o}C for 2 hours.

AII.1.2 Support Oxidation

1. Place in oven; ramp temperature up from 40^{o}C to 550^{o}C at a rate of 5^{o}C/min.
2. Hold at 550^{o}C for 12 hours
3. Ramp temperature back down from 550^{o}C to 40^{o}C at a rate of 5^{o}C/min
4. Hold at 40^{o}C to allow membrane to cool.

AII.2 Palladium Deposition

AII.2.1 Membrane Activation

1. Place support in graduated cylinder of fresh $SnCl_2$ solution for 5 min.
2. Remove and gently dip in cylinder of clean DI water for 2 min.
3. Remove and place in cylinder of DI water for 3 min.
4. Remove and rinse in DI water for 1 minute.
5. Place support in cylinder of fresh $PdCl_2$ solution for 5 min.
6. Remove and place support in fresh 0.1 M HCl solution for 2 min.

7. Remove and place in cylinder of fresh Di water for 3 min.
8. Remove and rinse in DI water for 1 min.
9. Repeat steps 1-8 5 more times for a total of 6 sequences.

AII.2.2 Electroless Plating

1. Wrap tubing with Teflon tape
2. Wash supports with DI water
3. Heat up water bath to 60^{o}C
4. Fill graduated cylinder with 70 mL of $Pd(NH_3)_4Cl_2$ solution and heat in water bath
5. Dip supports quickly into HCl and then back into DI
6. Mix 0.4mL of N_2H_4 with the $PdCl_2$
7. Place support into graduated cylinder and allow to sit in water bath for 90 min
8. While support is being plated, place a graduated cylinder with DI water into the heated bath along with a graduated cylinder with $Pd(NH_3)_4Cl_2$[1].
9. When 90 min is up, take support out and place into DI heated DI water
10. Rinse for 1-2 min
11. Add 0.4 mL of N_2H_4 to the next plating solution
12. Remove from DI and place into the next plating solution and let sit for another 90 min.
13. Repeat 7-12 as many times as needed.
14. Remove Teflon tape and place into the oven
15. Heat at 120^{o}C for 2-4 hrs

AII.2.3 Vacuum Plating

1. Follow steps 1-6 in electroless plating procedure
2. Place support in graduated cylinder and attach vacuum hose to the end of the support
3. For the first vacuum plating start vacuum at 0.25-0.5 bar for 30 minutes and then increase vacuum to maximum.
4. Allow support to sit in plating solution for 90 min
5. While support is being plated, place a graduated cylinder with DI water into the heated bath along with a graduated cylinder with either $Pd(NH_3)_4Cl_2$ solution of $AgNO_3$ depending on the next plating layer
6. After 90 min, remove from cylinder and dip in DI
7. Repeat 1-6 as many times as needed
8. Remove Teflon tape

[1] A solution of $AgNO_3$ was used alternately with the $Pd(NH_3)_4Cl_2$ solution during the generation of the BMML on the uncoated stainless steel support.

9. Place in the oven at 120^{o}C for 2-4 hrs

AII.3 Mechanical Membrane Modification

1. Place membrane in lathe and turn on
2. Using a long thin rectangular piece of 1200 grit sandpaper, slowly apply pressure to the membrane while holding the ends of the paper.
3. Move sandpaper up and down the membrane until desired results are obtained
4. Remove membrane from lathe and place in a graduated cylinder with acetone
5. Put graduated cylinder into sonic bath for 10 min
6. Remove and place in a graduated cylinder with isopropyl alcohol for 5 min
7. Remove and place in the oven to dry

Appendix III Plating history and helium flux data for USS membrane

Table 4: Raw helium flux data for USS Membrane

Bare SS Membrane (Lester)										
Notes:			P(psia)	P(psig)	(atm)	flux (m3/m2h)				
Bare SS Membrane			17.98	3.28	0.22	82.2				
Pre-cleaning			20.48	5.78	0.39	151.4				
Date:	**3-Nov-08**		22.98	8.28	0.56	226.3				
Mass:	**138.43**	**g**	27.98	13.28	0.90	382.7				
			32.99	18.29	1.24	553.9				
Notes:			P(psia)	P(psig)	(atm)	flux (m3/m2h)				
Bare SS Membrane			18.01	3.31	0.23	85.9				
Post-cleaning			23	8.3	0.56	231.3				
"Cleaned"			28.01	13.31	0.91	397.1				
Date:	**5-Nov-08**		33	18.3	1.24	568.8				
Mass:	**138.43**	**g**	30.5	15.8	1.07	478.4				
Notes:			P(psia)	P(psig)	(atm)	flux (m3/m2h)				
Bare SS Membrane			18.01	3.31	0.23	87.7				
Post-oxidation			22.98	8.28	0.56	233.9				
			27.99	13.29	0.90	397.1				
Date:	**6-Nov-08**		33.01	18.31	1.25	584.7				
Mass:	**138.43**	**g**	30.49	15.79	1.07	489.5				
Notes:			P(psia)	P(psig)	(atm)	flux (m3/m2h)	$th_{plating}$ (m)	$th_{plating}$ (um)	th_{total} (um)	
Bare SS Membrane			18	3.3	0.22	74.6	0.00	13.05	13.05	
Post-Plating 1			23.01	8.31	0.57	198.6				
(Pd-Ag-Pd-Ag-Pd)			28.02	13.32	0.91	334.1				
Date:	**14-Nov-08**		33.01	18.31	1.25	478.4				
Mass:	**138.77**	**g**	35.49	20.79	1.41	553.9				
Mechanical Treatment (Sanding)										
Notes:			P(psia)	P(psig)	(atm)	flux (m3/m2h)	$th_{plating}$ (m)	$th_{plating}$ (um)	th_{total} (um)	
Bare SS Membrane			18	3.3	0.22	104.7	0.00	-1.92	11.13	
Post-Sanding 1			23	8.3	0.56	191.3				
			27.99	13.29	0.90	323.8				
Date:	**17-Nov-08**		30.51	15.81	1.08	397.1				
Mass:	**138.72**	**g**	33.02	18.32	1.25	467.7				
Notes:			P(psia)	P(psig)	(atm)	flux (m3/m2h)	$th_{plating}$ (m)	$th_{plating}$ (um)	th_{total} (um)	
Bare SS Membrane			18.01	3.31	0.23	25.7	0.00	10.35	21.46	
Post-Plating 2			23.03	8.33	0.57	69.7				
(Pd x 5)			28.02	13.32	0.91	119.6				
Date:	**24-Nov-08**		33.02	18.32	1.25	175.4				
Mass:	**138.99**	**g**	40	25.3	1.72	263.1				
Mechanical Treatment (Sanding)										
Notes:			P(psia)	P(psig)	(atm)	flux (m3/m2h)	$th_{plating}$ (m)	$th_{plating}$ (um)	th_{total} (um)	
Bare SS Membrane			39.95	25.25	1.72	50.3	0.00	1.15	22.64	
Post-Plating 3			35.01	20.31	1.38	38.7				
(Pd x 4)			19.95	5.25	0.36	7.7				
Date:	**5-Dec-08**		21.99	7.29	0.50	12.2				
Mass:	**139.02**	**g**	25.05	10.35	0.70	17.3				
			23.99	9.29	0.63	16.4				

Notes:			P(psia)	P(psig)	(atm)	flux (m3/m2h)		$th_{plating}$ (m)	$th_{plating}$ (um)	th_{total} (um)
Bare SS Membrane			19.96	5.26	0.36	0.1		0.00	13.43	36.07
Post-Plating 4			25.05	10.35	0.70	0.3				
(Pd x 3 (reg) + x 1 (vacuum))			30.33	15.63	1.06	0.6				
Date:	**9-Dec-08**		34.65	19.95	1.36	0.8				
Mass:	**139.37**	**g**	39.99	25.29	1.72	1.2				
Notes:			P(psia)	P(psig)	(atm)	flux (m3/m2h)		$th_{plating}$ (m)	$th_{plating}$ (um)	th_{total} (um)
Bare SS Membrane			29.53	14.83	1.01	0.1		0.00	9.58	45.60
Post-Plating 5			34.21	19.51	1.33	0.1				
(Pd x 2 (vacuum))			39.42	24.72	1.68	0.2				
Date:	**11-Dec-08**		44.4	29.7	2.02	0.3				
Mass:	**139.62**	**g**	26.31	11.61	0.79	0.1				
Mechanical Treatment (Sanding)										
Notes:			P(psia)	P(psig)	(atm)	flux (m3/m2h)		$th_{plating}$ (m)	$th_{plating}$ (um)	th_{total} (um)
Bare SS Membrane			30.24	15.54	1.06	0.0		0.00	8.05	44.08
Post-Plating 6			35.2	20.5	1.39	0.0				
(Pd x 2 (vacuum))			40.34	25.64	1.74	0.1				
Date:	**15-Dec-08**		45.29	30.59	2.08	0.1				
Mass:	**139.58**	**g**	48.68	33.98	2.31	0.1				
			25.06	10.36	0.70	0.0				
Notes:			P(psia)	P(psig)	(atm)	flux (m3/m2h)		$th_{plating}$ (m)	$th_{plating}$ (um)	th_{total} (um)
Bare SS Membrane			44.18	29.48	2.00	0.0		0.00	3.45	47.54
Post-Plating 7			47.05	32.35	2.20	0.0				
(Pd x 2 (vacuum))			37.58	22.88	1.56	0.0				
Date:	**16-Dec-08**		35.71	21.01	1.43	0.0				
Mass:	**139.67**	**g**								
Notes:			P(psia)	P(psig)	(atm)	flux (m3/m2h)		$th_{plating}$ (m)	$th_{plating}$ (um)	th_{total} (um)
Bare SS Membrane			46.79	32.09	2.18	0.0		0.00	3.07	50.63
Post-Plating 7										
(Pd x 2 (vacuum))										
Date:	**16-Dec-08**							m	um	
Mass:	**139.75**	**g**						5.0648E-05	50.65	

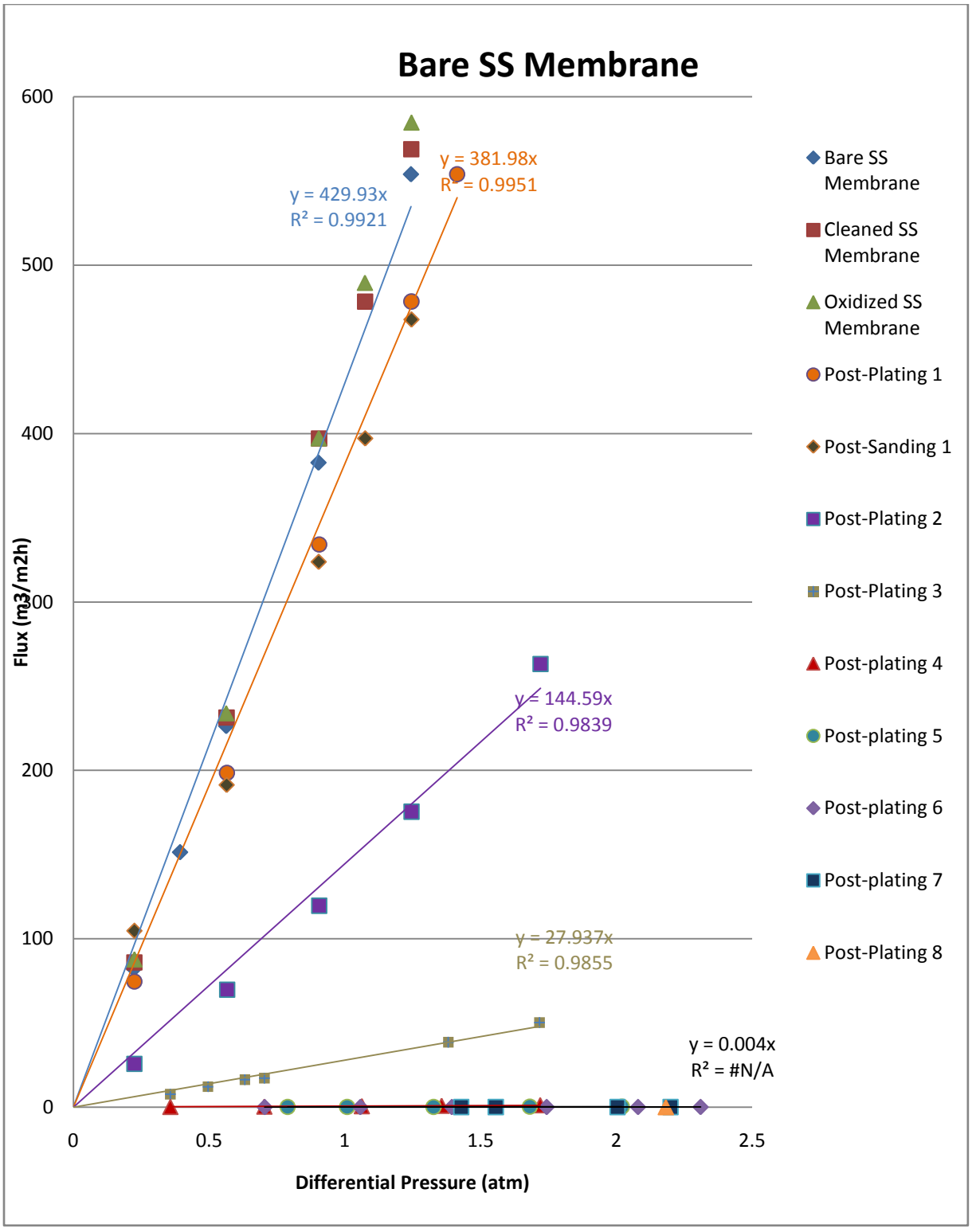

Figure 9: Helium flux data for USS support

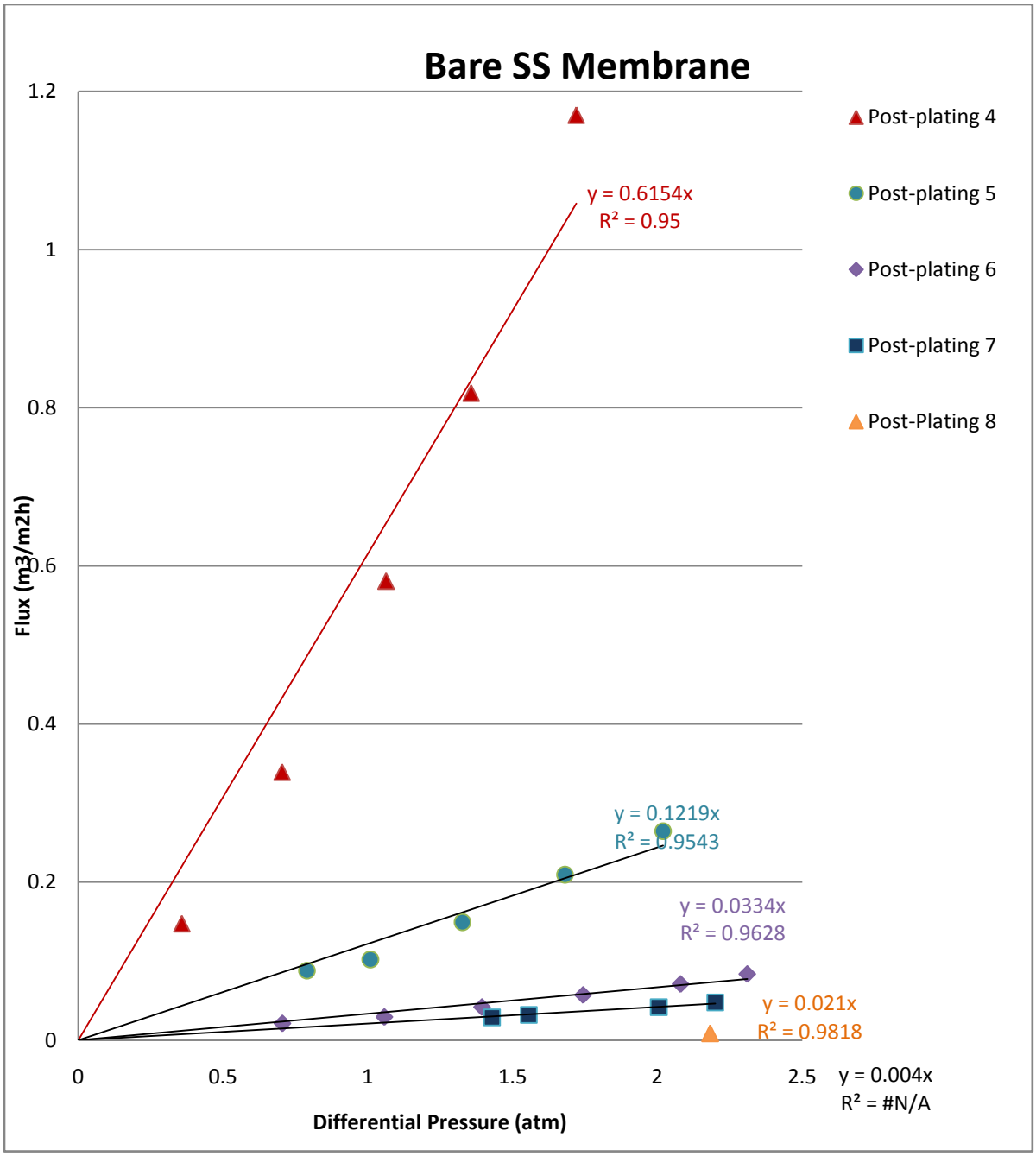

Figure 10: Helium flux data for USS support (platings 5-8)

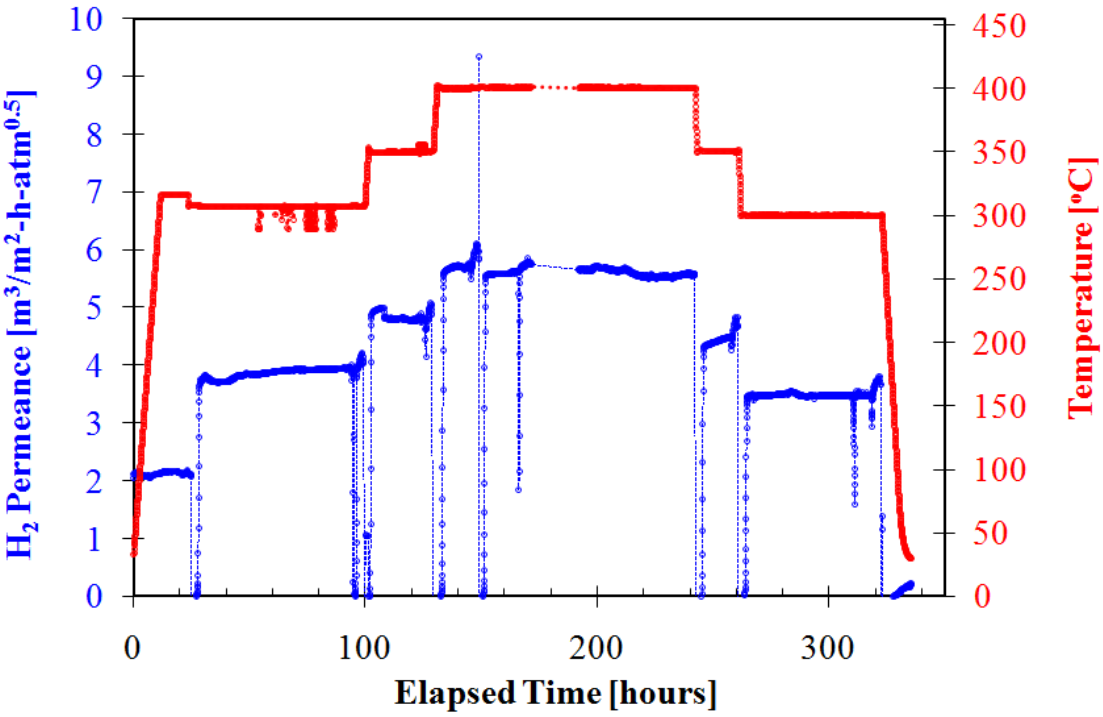

Figure 11: H_2 Permeance vs. Temperature vs. Elapsed Time for USS/Pd membrane

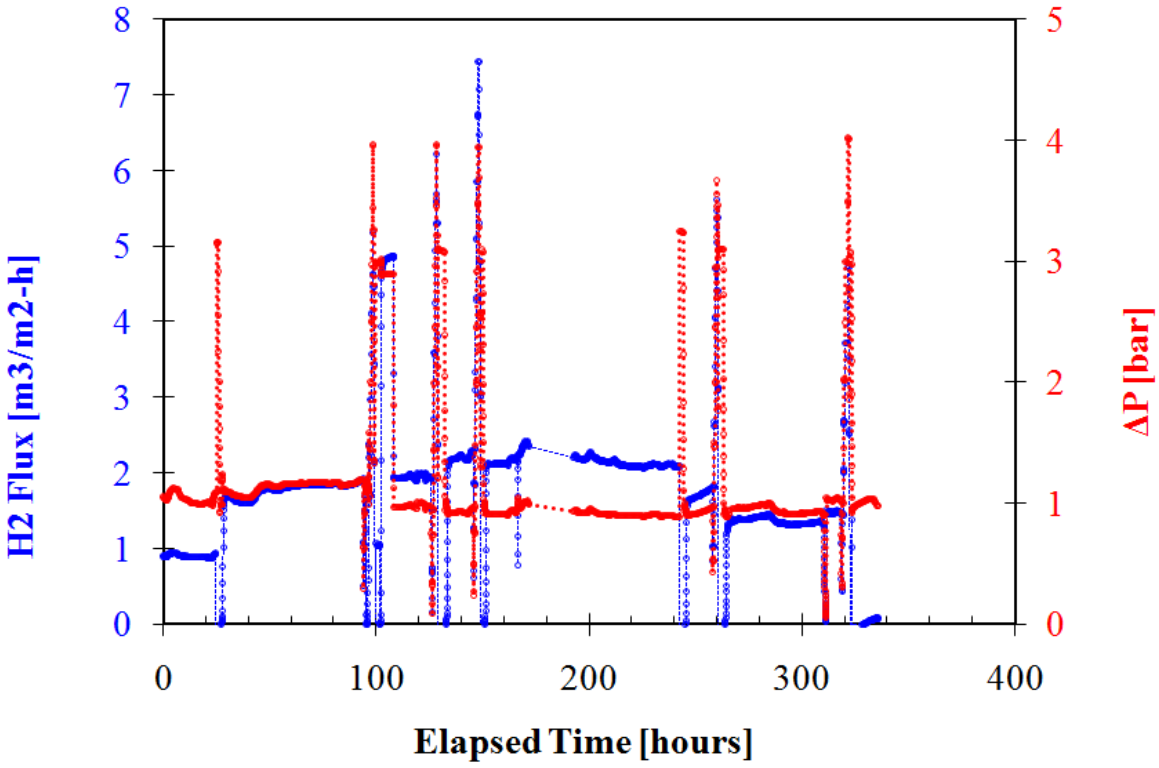

Figure 12: H_2 flux vs. Time for USS/Pd membrane

Appendix IV Plating history and helium flux data for ZrO_2 membrane

Table 5: Raw helium flux data for ZrO_2 Membrane

Zirconium Oxide Membrane (Amanda)										
Notes:			P(psia)	P(psig)	(atm)	flux (m3/m2h)				
Zirconium Oxide Membrane			17.99	3.29	0.22	30.9				
Pre-cleaning			23.01	8.31	0.57	86.6				
Date:	**3-Nov-08**		28.03	13.33	0.91	144.2				
Mass:		**g**	33	18.3	1.24	202.4				
			37.97	23.27	1.58	263.1				
			42.98	28.28	1.92	328.9				
			48.01	33.31	2.27	397.1				
Notes:			P(psia)	P(psig)	(atm)	flux (m3/m2h)				
Zirconium Oxide Membrane			18	3.3	0.22	31.0			0	0
Post-cleaning			23.02	8.32	0.57	81.1				
"Cleaned"			28	13.3	0.90	133.2				
Date:	**5-Nov-08**		32.99	18.29	1.24	186.3				
Mass:	**140**	**g**	38.01	23.31	1.59	241.9				
			42.94	28.24	1.92	300.7				
Notes:			P(psia)	P(psig)	(atm)	flux (m3/m2h)	$th_{plating}$ (m)	$th_{plating}$ (um)	th_{total} (um)	
Zirconium Oxide Membrane			22.89	8.19	0.56	0.05	0.00	2.69	2.69	
Post-Plating 1			27.98	13.28	0.90	0.08				
(Pd-Ag) [electronic meter]			32.95	18.25	1.24	0.11				
Date:	**14-Nov-08**		37.28	22.58	1.54	0.15				
Mass:	**140.07**	**g**	41.42	26.72	1.82	0.18				
			44.34	29.64	2.02	0.20				
Notes:			P(psia)	P(psig)	(atm)	flux (m3/m2h)	$th_{plating}$ (m)	$th_{plating}$ (um)	th_{total} (um)	
Zirconium Oxide Membrane			33.2	18.5	1.26	0.07	0.00	0.00	2.69	
Post-Plating 2			38.25	23.55	1.60	0.09				
(Pd x1) [electronic meter]			42.53	27.83	1.89	0.11				
Date:	**24-Nov-08**		47.48	32.78	2.23	0.14				
Mass:	**140.07**	**g**	40.02	25.32	1.72	0.10				
Notes:			P(psia)	P(psig)	(atm)	flux (m3/m2h)	$th_{plating}$ (m)	$th_{plating}$ (um)	th_{total} (um)	
Zirconium Oxide Membrane			40.3	25.6	1.74	0.05	0.00	-0.38	2.30	
Post-Plating 3			43.17	28.47	1.94	0.06				
(Pd x4) [electronic meter]			46.15	31.45	2.14	0.07				
Date:	**5-Dec-08**		48.19	33.49	2.28	0.08				
Mass:	**140.06**	**g**								
Notes:			P(psia)	P(psig)	(atm)	flux (m3/m2h)	$th_{plating}$ (m)	$th_{plating}$ (um)	th_{total} (um)	
Zirconium Oxide Membrane				-14.7	-1.00	#DIV/0!	0.00	4.22	6.91	
Post-Plating 4										
(Pd x2 vacuum)										
Date:	**5-Dec-08**									
Mass:	**140.17**	**g**								

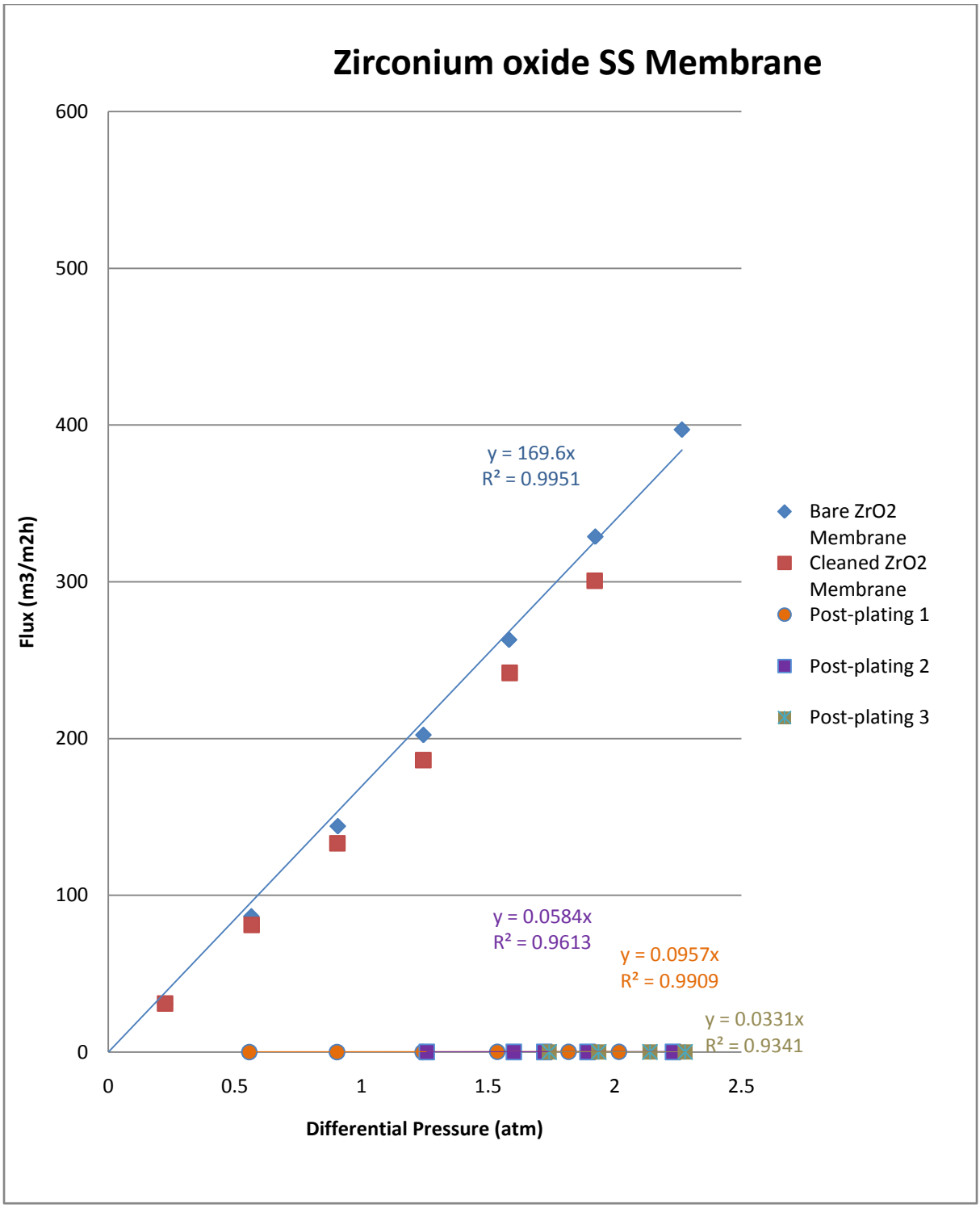

Figure 13: Helium flux data for ZrO_2 coated support

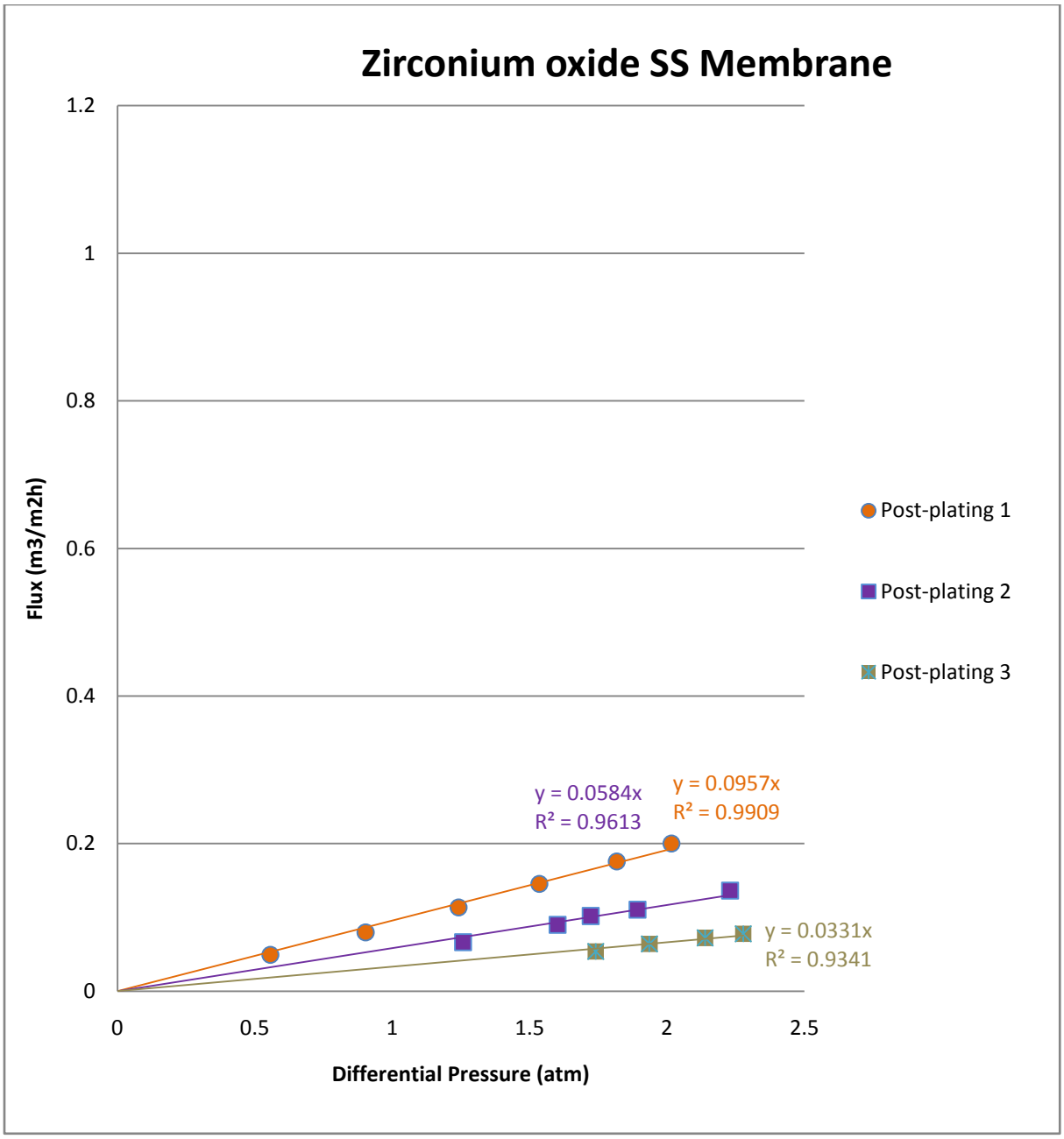

Figure 14: Helium flux data for ZrO_2 coated support (platings 1-3)

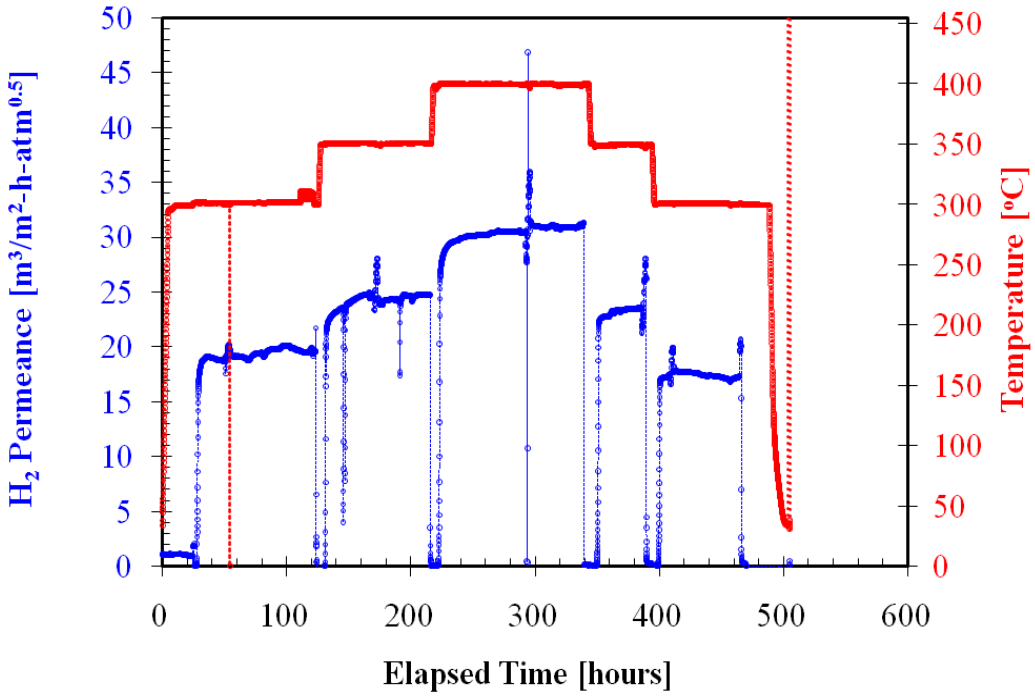

Figure 15: Corrected H_2 Permeance vs. Temperature vs. Elapsed Time for ZrO_2/Pd membrane

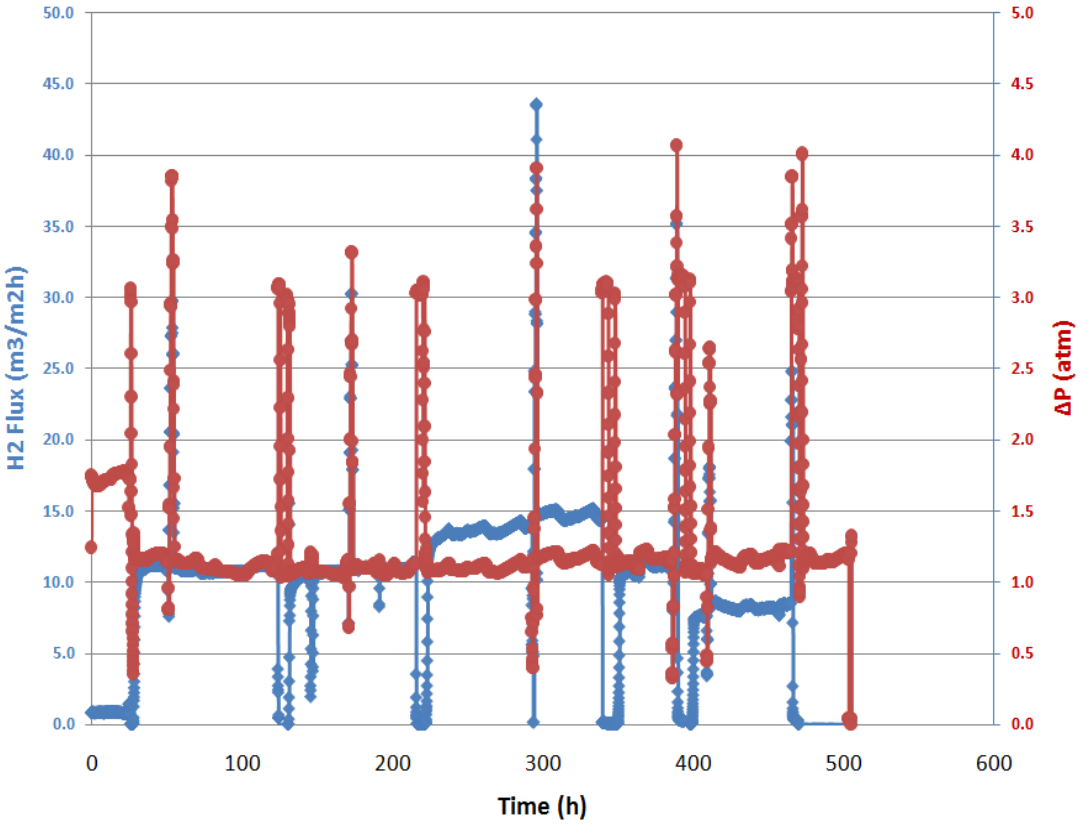

Figure 16: H_2 flux vs. Time for ZrO_2/Pd membrane